Simulation of 3D Temperature Fields of Sensors Supported by 2D IR Camera Images of Sensors' Surface Temperatures

PAVEL NEVRIVA , ZDENEK MACHACEK, JAN KRNAVEK
Department of Measurement and Control
VSB Technical University of Ostrava
17. listopadu 15, 708 33 Ostrava-Poruba
CZECH REPUBLIC
pavel.nevriva@vsb.cz, http://www.vsb.cz

Abstract: - In this paper, the calculation of temperature fields inside sensors' bodies is discussed. The temperature of a sensor is a function of time and spatial coordinates. Structures of mathematical models describing the temperature fields depend on the environment in which sensors operate. In this paper, temperature fields in sensors are described by the Fourier partial differential equation. Mathematical model of the particular sensor has many parameters which are known with limited accuracy. To upgrade this accuracy, the physical model incorporating both the analyzed sensor and the ambient conditions similar to the real ones is built. Mathematical model is constructed and calculated to solve tasks described by the physical model. Differences between analytical and experimental results are used for an adaptive correction of parameters of the mathematical model. In this paper, differences between models are evaluated from differences between surface temperatures of the sensors. At the physical model, sensor's surface temperature is measured by the infrared camera. At the mathematical model, sensor's temperature is obtained solving the Fourier partial differential equation by the finite element method. It is calculated by the ANSYS Workbench software. Numerical values of sensors' surface temperatures from both models can be displayed as images. To compare the experimental and analytical results, images generated by the IR camera are transformed by a set of image processing functions. Both the general method and the case study results obtained on the complex problem of the analysis of the heat transfer dynamics of the motor oil level gauge are presented.

Key-Words: - simulation, image processing, finite element methods, sensors.

1. Introduction

Sensors are important part of most automatic systems. Thermal load of sensors affects the accuracy of measurement and control.

In this paper, the analysis of temperature fields in sensors is discussed. The development of their mathematical models, their numerical calculation and experimental verification is shown.

Temperature fields in sensors are usually described by the Fourier partial differential equation. It is rather difficult to accomplish accurate mathematical models of sensors built in actual operating conditions. There is a problem with the description of ambient conditions of the sensor, resulting to problems with the definition of initial and boundary conditions of the Fourier partial differential equation. There could be also problems with verification of the model. Therefore, the physical models incorporating both the analyzed sensors and the ambient conditions similar to the real ones are built. Mathematical models are then constructed and calculated to solve the tasks described by the physical models.

To solve the Fourier partial differential equation, complexity of sensor construction usually results in application of numerical methods and simulation techniques. The Fourier partial differential equation can be calculated numerically with a great accuracy. Validity of the mathematical model of a sensor depends on accuracy of physical parameters describing a sensor, sensor's setup and a sensor's ambient.

In most practical applications of theory the solution of Fourier partial differential equation leads to a unique time development of temperature field at a three-dimensional surface of a sensor. To find the congruence of a mathematical model with an actual sensor, the surface temperature calculated by the mathematical model is compared with temperature measured at the surface of the actual sensor.

In experiments reported in this paper, the basic measurement of temperature was made by the by the IR

camera. In this paper, the image processing functions filter numerical data generated by IR camera and synchronize them with data obtained from analytical model.

2 Physical models of sensors

Physical models are placed in laboratory. Physical models match the sensors location under operating conditions. In physical models, actual sensors operate in defined environment and under defined heat inputs. Mathematical models of sensors are constructed to simulate tasks specified for the physical models. Plausibility of mathematical models is tested by measurements accomplished at sensors which are parts of physical models.

In the presented study, the ambient conditions in laboratory were stabilized. Temperature of the ambient air in laboratory was stabilized to 294.2K (21°C). The tong-lasting accurate temperature stabilization of the ambient conditions in the laboratory was one of the difficult problems of the measurement.

Fluids were homogeneous in physical models. There was a natural convection between fluids and solids. The forced convection was held on value near to zero. For sensors cooled by ambient air such situation represents the worst case.

The residual forced convection contributes to correction of heat transfer coefficients α of the mathematical model, see below.

Measurement of the sensor's surface temperature was carried out by individually calibrated IR camera. The surface of sensor was blackened to have the total coefficient of emissivity $\varepsilon = 0.96$. IR camera was connected to the computer. Its output was saved as the matrix of numerical data. It was displayed as IR camera color image. The standard color spectrum of IR camera pictures was transformed into the gray scale for monochrome reproduction in this paper. All IR camera images were processed by MATLAB image processing functions, see below Paragraph 6. Note, that at every measurement several additional temperatures were also measured by sensors with bimetal thermometers and resistance thermometers.

3. Mathematical models of sensors

The analysis of the heat transfer often combines three basic physical principles: conduction, convection, and radiation [5].

Conduction is a form of heat transfer characteristic for solids. Conduction could perform also in fluids. Fluids must be in absolute inaction. One differentiates stationary conduction and non-stationary conduction. In this task we deal with non-stationary conduction.

Temperature

$$T = T(x, y, z, t)\ [\mathrm{K}]$$

of all solid parts of the sensor is given by the Fourier partial differential equation

$$\frac{\partial T}{\partial t} = A\left(\frac{\partial^2 T}{\partial x^2} + \frac{\partial^2 T}{\partial y^2} + \frac{\partial^2 T}{\partial z^2}\right) \qquad (1)$$

where

t is time [s]

(x, y, z) is vector of spatial variables $[\mathrm{m}, \mathrm{m}, \mathrm{m}]$

$$A = \frac{\lambda}{\rho c_p}\ [\mathrm{m^2 s^{-1}}]$$

Parameters in coefficient $A = \lambda / \rho c_p$ represent the constructional materials of the sensor. Their values are functions of temperature and spatial variables. Here

λ is the thermal conductivity [$\mathrm{Wm^{-1}K^{-1}}$],
ρ is the density [$\mathrm{kg\ m^{-3}}$]
c_p is the specific heat capacity [$\mathrm{J\ kg^{-1}K^{-1}}$]

of individual structural components.

To obtain unique solution of the Fourier partial differential equation, the initial and boundary conditions have to be introduced. According to three basic heat transfer problems the boundary conditions of Fourier partial differential equation are ordinarily divided into three basic kinds.

The boundary condition of the first kind is usually given by the temperature $T = T(x, y, z, t)$ of a given surface of a body.

The boundary condition of the second kind results from a source of density of heat flow rate $q = q(x, y, z, t)$ at the surface of the body.

The boundary condition of the third kind is defined by a given ambient temperature. It has the form

$$q = \alpha(T_A - T_S) \qquad (2)$$

where

q is the density of heat flow rate [$\mathrm{Wm^{-2}}$]
α is the heat transfer coefficient [$\mathrm{Wm^{-2}K^{-1}}$]
T_A is the ambient temperature [K]
T_S is the temperature of solid surface [K]

Note, that among relations used for calculation of boundary conditions belong also equations comprising both the heat transfer caused by radiation energy and the heat interface between two solids.

Solution of the Fourier partial differential equation starts from the initial conditions, describing the temperatures of the sensor and the sensor's setup at the time $t = 0$.

The Fourier partial differential equation is solved for initial and boundary conditions corresponding to the particular physical problem.

4 Comparison of models

Camera scans the sensor's surface and measures the time sequence $\mathbf{T}_p$ of $N+1$ digital $I \times J$ images $T_{p,n}(i,j)$. $T_{p,n}(i,j)$ is the sensor's surface temperature. Coefficient $n = 0,1,2,\cdots N$ defines the sampling time $t_S = nT_S$ where T_S is the constant camera sampling interval. Parameters i, j are coordinates of image pixel row and column position, $i = 1,2,\cdots I$, $j = 1,2,\cdots J$. At every IR camera image there is selected an area A suitable for comparison of models. It defines the $r \times s$ matrix $\boldsymbol{T}_{p,n}$.

Mathematical model generates the corresponding sequence $\mathbf{T}_m$ of $N+1$ digital images $T_{m,n}(i,j)$, $n = 0,1,2,\cdots N$ with sensor's surface temperatures. Both sets of images are processed and synchronized. At every image the $r \times s$ matrix $\boldsymbol{T}_{m,n}$ related to $\boldsymbol{T}_{p,n}$ is derived. To compare the surface temperatures the measurement results are projected on the plane. Area A suitable for comparison of models has to be selected with regards to the minimal distortion of measurement.

In example reported below, the sampling interval $t_S = 5\text{s}$ was selected. The time sequences contained $N = 800$ images of $I = 240,\ J = 320$. To increase the measurement accuracy, the measurements were taken for two sensors of the same butch several times.

Resolution of IR camera was better then $0.1\,\text{K}$. The absolute difference between temperatures in individual measurement runs was about $0.4\,\text{K}$. It indicates measurement with sufficient precision. A comprehensive statistical analysis of raw data was therefore omitted here. An average measurement run was taken as an exact one.

Both, the physical and the mathematical model were set at the same initial temperature. Then, both models were agitated by the identical heat step input. Temperatures in models grew into new steady state values.

The difference between the measured and calculated temperature fields represents the accuracy of the mathematical model. To simplify the rectification of parameters of the mathematical model, transients derived from values calculated by mathematical model may be compared with those derived from values measured at the physical model. Such transients may be for example discrete-time signals that represent the maximal temperature $T_p[n]$ and the maximal temperature $T_m[n]$, see example below. The comparison of transient waveforms results in determination of new values of physical parameters of mathematical model which leads to a new iteration in an optimization process and to new values of transients. To control the iteration process, the artificial intelligence fuzzy knowledge based system was successfully applied [8].

To compare the structure of the mathematical model, the correlation coefficient $r_n = r_{m,p,n}$ between the matrix $\boldsymbol{T}_{m,n}$ and the matrix $\boldsymbol{T}_{p,n}$ can be calculated.

5 Level gauge analysis

As a case study, the analysis of the heat transfer dynamics of the motor oil level gauge is presented in this paper. The geometrical model the of oil level gauge is shown in Figure 1.

Fig.1. Geometrical model of oil level gauge.

The simplified composition of the simulated sensor find in Figure 2.

Its housing contains two principal parts. The foot is made from duralumin. The upper part is made from plastic. The dominant element of plastic part is the narrow hollow plastic stem.

The stem is immersed into the oil in the motor car oil pan case. Inside the column, there is the filament

stretched alongside its wall.
The filament is heated by the train of electrical impulses. Its resistance is changing due its temperature and depends on its cooling by oil.

The intensity of cooling depends both on the level and temperature of oil the filament is immersed in. In addition, the sensor also has to measure the temperature of the oil.

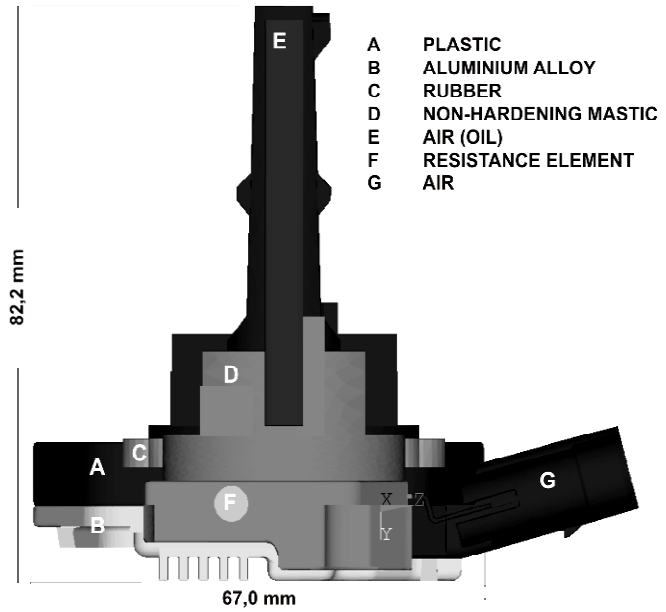

Fig. 2. Oil level gauge. The simplified composition of the sensor.

The centre of the housing covers electronics that controls and evaluates all functions of sensor. The rest of the sensor's body is filled in by the non-hardening mastic.

In the service, the sensor is connected by three screws to the automobile oil pan case and is attached to the motor car board computer.

The body of the sensor is spuriously heated by oil and by the self-heating. The duralumin part serves as a cooler of the sensor's electronics.

The undesirable heating of the sensor makes problems to a sensor's electronics. The mathematical model of the temperature load of oil level gauge was constructed. In this paper, the study of the temperature fields resulting from self-heating is presented.

The power loss of the electronics of the oil level gauge is about 100 mW. It is small value when compared with the power transferred to the sensor from the hot oil in the oil pan case and the direct analysis of the corresponding increase of temperature at the sensor's surface may be beyond an accuracy of measurement.

On the other hand, the increase of temperature near its source, it is the increase of temperature of electronics due its power loss, cannot be neglected.

To be able to verify the mathematical model of sensor's self-heating, the physical model of the modified sensor was constructed as follows: actual electronics of the sensor was replaced by the forty times larger energy source.

We have a representative task where the analysis of a process by measurement is difficult and where the mathematical simulation of the physical process can be very useful.

The resistor of the defined geometry supplied by 4W power was set into the position of the sensor's electronics.

The replacement enables to verify the mathematical model of the sensor by measurement. Actual calculations are then made for the actual thermal load.

The detail of the physical model is shown in Figure 3. The figure maps the cylindrical resistor situated inside the mastic supported by the bottom of the sensor.

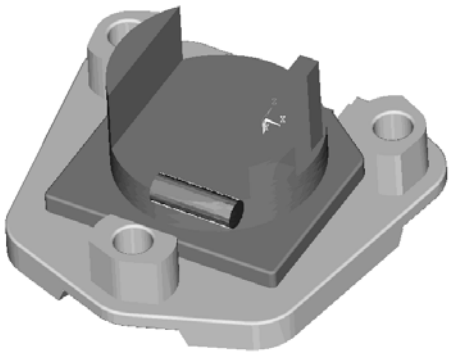

Fig. 3. Oil level gauge - detail of the physical model. Location of the heating resistor.

At laboratory, the sensor was connected to the automobile oil pan case. The mathematical model was constructed to solve the task described by the physical model. The schema of the physical model is shown in Figure 4.

Initial temperature of the level gauge and the associated parts of physical model were set at the stabilized constant value of ambient air of 294.2K.

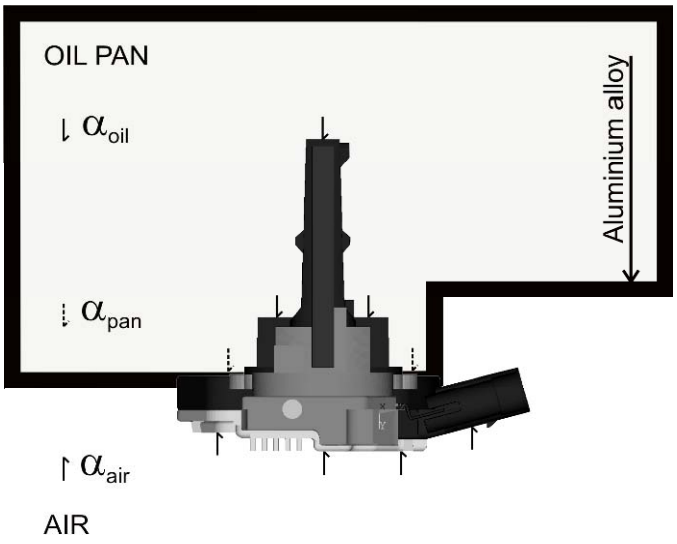

Fig.4. Physical model - oil level gauge in motor car oil pan case.

The development of temperature of the duralumin bottom level gauge cooler part calculated by the mathematical model was compared with that measured by an IR camera. The measurement setup is shown in Figure 5.

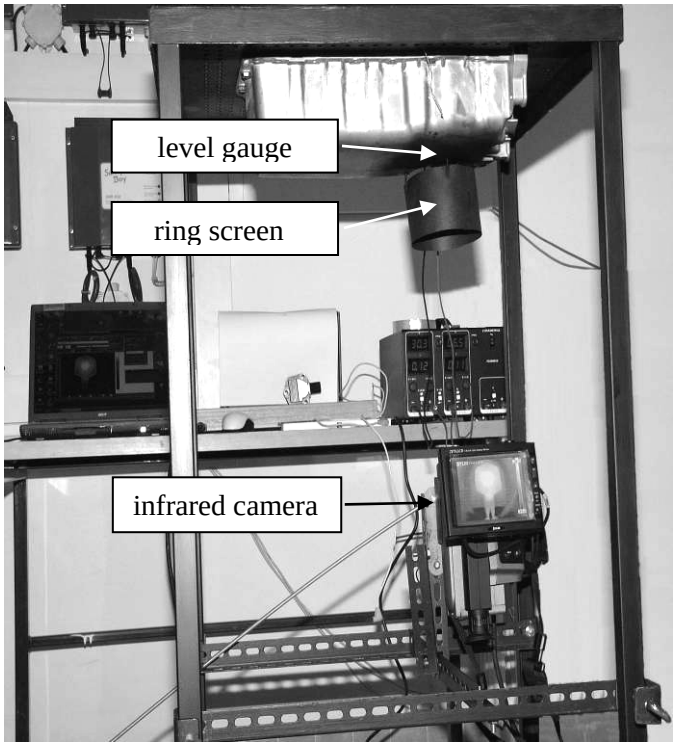

Fig. 5. Measurement setup, shield removed.

To avoid problems with reflection and to minimize the angle error, area A suitable for comparison of models was selected here with respect to the maximal square that can be embedded into the shape of sensor's cooler. Area A is the square that is coaxial to the maximal square and contains 0.64 of its area.

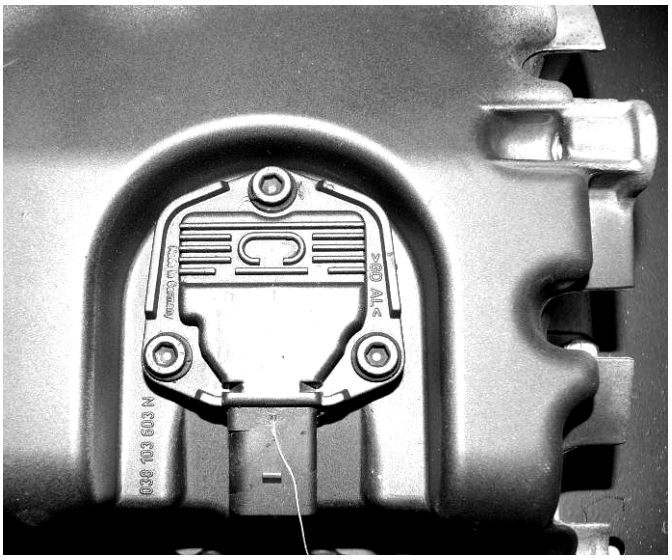

Fig.6. Oil level gauge attached to the oil pan case, view from below.

6 IR camera images processing

Figure 7 shows the original rough IR camera images $T_{p,n}$ of the level gauge cooler in 750 and 1500 s.

To compare results obtained by measurement those generated by ANSYS, the rough IR camera images were transformed by five basic image processing functions.

The first logical step was noise filtering. The noise in the image has its origin in a rough surface of sensor and real laboratory conditions. The disturbance occurs particularly due the air. To reject the noise, the image $T_p(i, j)$ was transformed by the two-dimensional Discrete Fourier transform

$$\tau_p(u,v) = \sum_{i=0}^{I-1}\sum_{j=0}^{J-1} T_p(i+1, j+1) e^{-\mathrm{j}\,2\pi\left(\frac{u\,i}{I}+\frac{v\,j}{J}\right)} \qquad (3)$$

The Fourier spectrum $\tau_p(u,v)$ was slightly filtered by the Gaussian low-pass filter. Images or measured data were filtered in the frequency domain. Filtering in the space domain leads to convolution and is also possible.

Note that the Gaussian image smoothing also prepares application of subsequent Canny's method of detection of edges.

The impulse response of the 2D Gaussian filter is given by

$$h(u,v)=\frac{1}{\sqrt{2\pi\sigma_u\sigma_v}}e^{-\frac{1}{2}\left[\frac{x^2}{\sigma_x^2}+\frac{y^2}{\sigma_y^2}\right]} \quad (4)$$

The frequency response of the 2D Gaussian Filter is given by

$$H(u,v)=\frac{1}{2\pi\sigma_u\sigma_v}e^{-\frac{1}{2}\left[\frac{u^2}{\sigma_u^2}+\frac{v^2}{\sigma_v^2}\right]} \quad (5)$$

where

$$\sigma_u=\frac{1}{2\pi\sigma_x},\quad \sigma_v=\frac{1}{2\pi\sigma_y}$$

The next step was to define the edge limits of the sensor. The Canny's edge detection method of threshold detection with respect to the picture gradient direction was selected for this purpose [1]. Method detects both the distinctive and indistinctive thresholds. The advantage of this method is its complexity and infallibility. The indistinctive thresholds detection helps to use the method to detect sensor's edges from the start of the heating process.

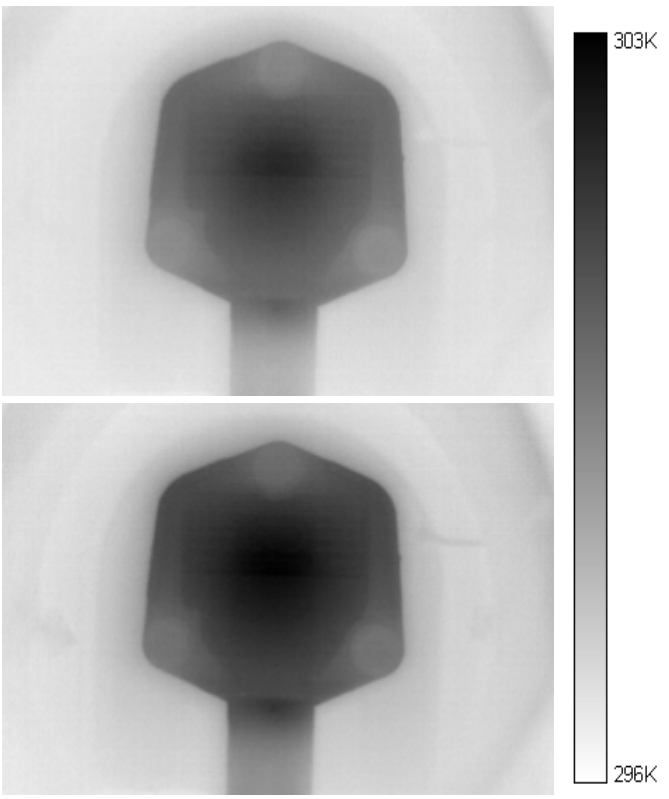

Fig. 7. Rough IR camera images of the level gauge cooler in 750 and 1500 s.

The disadvantage of this method is that its parameters have to be set very accurately. Here, parameters that determine the edges and filter dimensions were adjusted experimentally. The other disadvantage of Canny's method is its intricacy and the time consuming algorithms.

On the other hand, the IR camera images taken from the physical model are treated by this method only once and the total time the method occupies on computer is negligible when compared with the time that is spent for the iterative optimization of parameters of the mathematical model made by finite element method.

Filtered camera images of the level gauge cooler supplemented with sensor edge limits are shown in Figure 8.

The last step was to fix the IR camera images to those generated by the ANSYS graphical generator or with data calculated by mathematical model. The dimensions and relative position of both images has to correspond. Two points of intersection of three lines defined in the camera image were fixed to those at the mathematical model image.

The minor vibrations of IR camera are a cause for individual positioning of every camera image. This positioning is made only once. This is not a time consuming procedure.

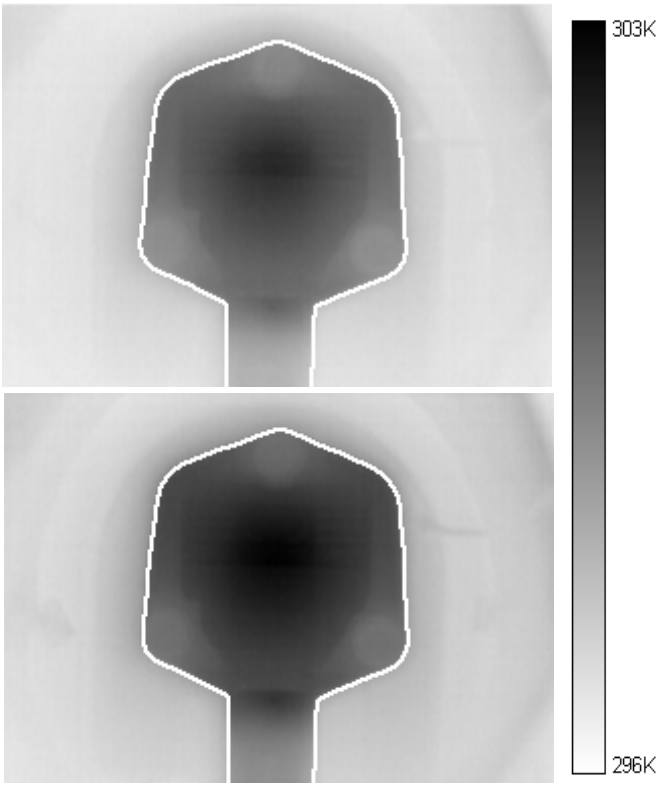

Fig. 8. Filtered IR camera images of the level gauge cooler in 750 and 1500 s. Sensor's edge limits are added

The images derived from the mathematical model are always generated in fixed position.

The consecutive step was the image background rejection. The resulting position of images was corrected by the correlation calculus.

The discrete temperature scaling was added to this logical procedure, see Figure 9. Average temperatures of the subfields are indicated. Images of that type may be illustrative but they mask the accuracy of data they represent. Compare Figure 13.

The infrared camera was set approximately 30 cm from the level gauge, see Figure 5. To obtain the representative results, the face plane of the cooler of the level gauge was set to be perpendicular to optical axis of camera. The surface of sensor's duralumin cooler was blacken to have the maximal and constant emissivity coefficient.

Parameters of the infrared camera:

Maximal sampling frequency:	1frame/s
Accuracy, calibrated:	0.2 K
Temperature resolution:	0.08 K
Image resolution:	240×320 pixels

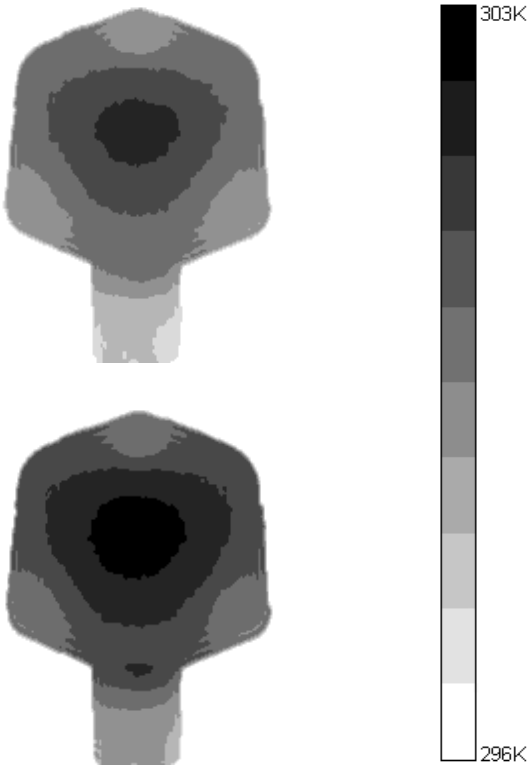

Fig. 9. IR camera images of the level gauge cooler in 750 and 1500 s. Discrete temperature scaling.

Figure 10 illustrates the resolution of measurement made by the infrared camera. It shows temperature differences at the lamellas of the sensor's fin cooler. Both, straight lamellas and the C-shaped lamella can be detected.

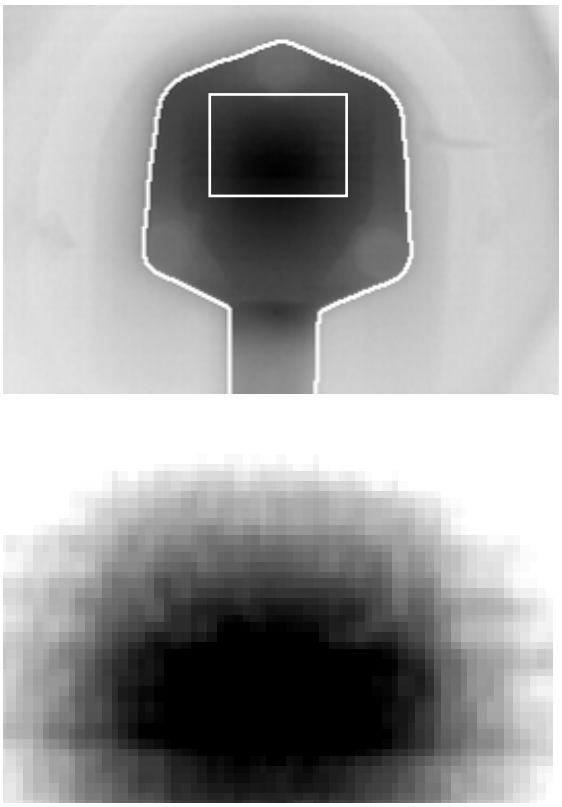

Fig. 10. Magnified IR camera image, Fig. 8b, reveals the structure of the sensor's fin cooler. Compare Figure 6.

7 Mathematical simulation results

The calculation of the equation (1) was made in the software product ANSYS Workbench 10 (about 180 000 elements). Automatic element size generation was selected. Figures 11 and 12 show the parts of the loose-meshed model compositions. At Figure 12, there are about 40 000 elements.

Initial conditions and boundary condition of the third kind were given by the temperature of the ambient air. The level gauge and the associated parts of physical model were set and located at the stabilized constant temperature of the ambient air of 294.2K.

The boundary condition of the second kind was given by the heat flux from the embedded resistance. It was defined by both the resistance geometry and the resistance power. The resistor was agitated by the constant power of 4W.

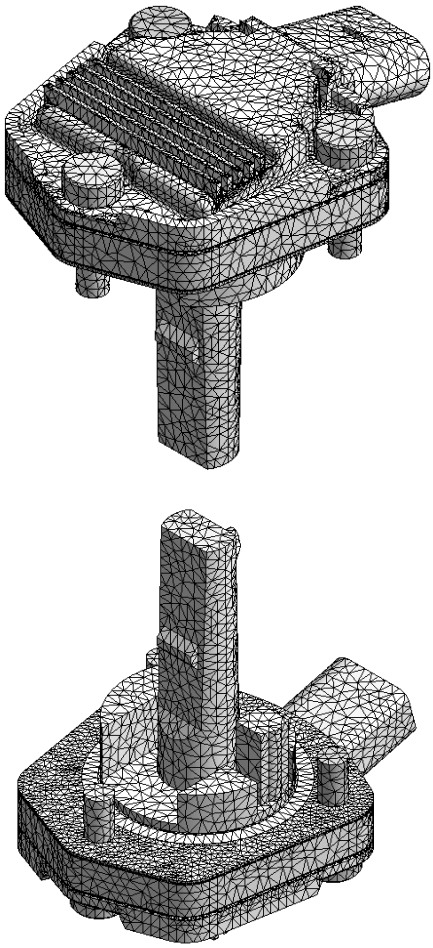

Fig.11. Meshed oil level gauge with bolts.

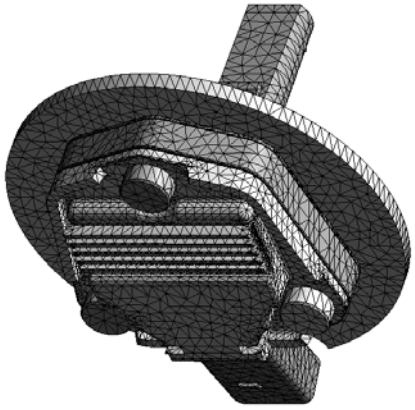

Fig.12. Meshed oil level gauge with bolts, seal and the section of the oil pan case.

Results presented in Figures 13, 14, and 15 were obtained by optimizing the heat transfer coefficient α between duralumin cooler and the air to obtain the zero difference between both maximal measured and maximal calculated steady-state temperatures in the sensor's cooler. The initial estimate of the heat transfer coefficients α is not accurate. Its actual value is affected by the residual forced convection. The principal reason for correction of heat transfer coefficients α is the fact that the actual values of the heat transfer coefficients α depend on materials, shapes, sizes and locations of surfaces they characterize.

Optimization of other parameters in Fourier partial differential equation would lead to minimization of difference between mathematical model and the physical model.

Sensor is a set of components. Geometrical drawings of the sensor parts, oil pan case, sealing rings, screws, etc. were prepared in Pro/Eng software. Material parameters λ, c_p, and ρ were defined for each component individually.

Figure 13 shows ANSYS generated temperatures calculated by the optimized mathematical model in 750 and 1500 s in a grey scale. Average temperatures of the subfields are indicated.

Figure 14 shows the ANSYS-generated temperature propagation in the longitudinal section of the level gauge body in the inverse gray scale. Maximal steady-state temperature measured at the sensor's cooler was

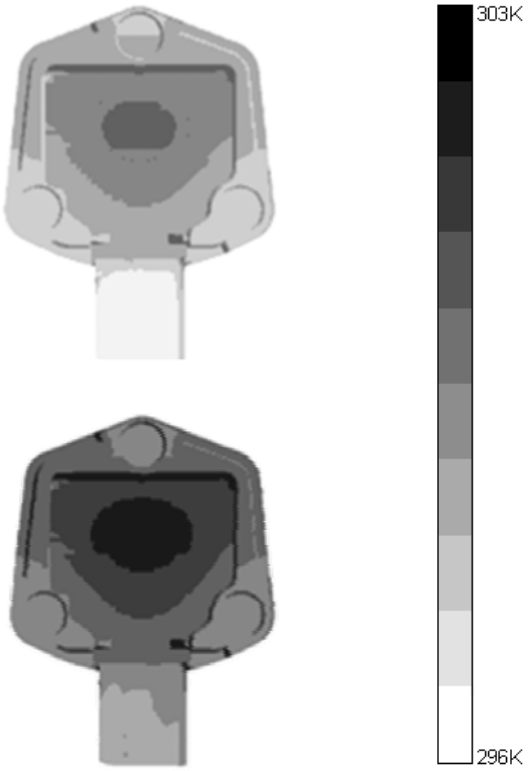

Fig. 13. Calculated temperature fields in 750 and 1500s. ANSYS-generated image, grey scale.

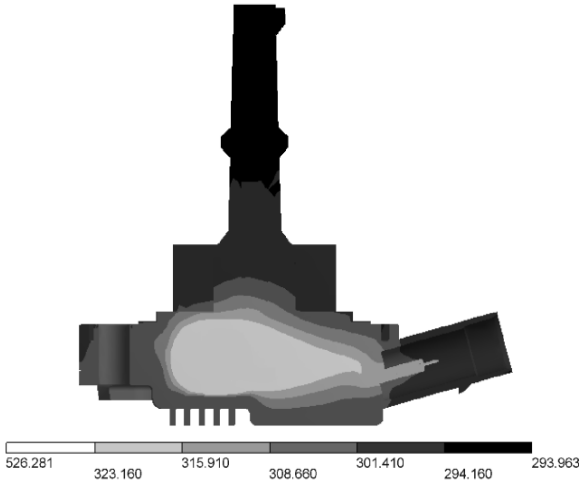

Fig. 14. Calculated temperature field, steady state. ANSYS-generated image, inverse grey scale.

302.2 K ± 0.2 K. Interval ± 0.2 K is given by the accuracy of the IR camera.

Figure 15 compares selected time responses of the physical and mathematical model.

In Figure 15, the measured temperature is shown as the function of time. To model this function, the regression analysis using the least square method was applied.

The value of the area correlation coefficient of the matrix $\boldsymbol{T}_{m,N}$ and the matrix $\boldsymbol{T}_{p,N}$ was $r_N = 0.93$.

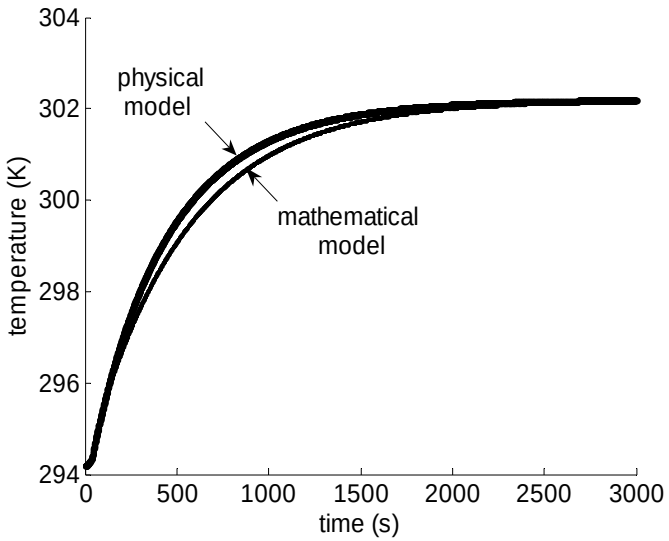

Fig.15. Maximal measured and calculated temperatures at the sensor's cooler

8 Conclusion

Sensors are part and parcel of most automatic control systems.

In this paper, the field tested method of analysis of temperature fields of sensors is presented.

Mathematical model of sensor's temperature field based on Fourier partial differential equation is built up. Accuracy of the mathematical model depends on accuracy of physical parameters describing both sensor and sensor's ambient. To set parameters of the mathematical model, the laboratory physical model incorporating both the actual sensor and the sensor's real working assembly is constructed. The validation of the mathematical model is based on comparison of calculated surface temperature with that measured by the infrared camera on physical model. Image processing principles are used for models comparison.

The method takes advantage of the continuous measurement of the surface temperature of the sensor by the infrared camera. Differences between analytical and experimental results are used for adaptive correction of parameters of the mathematical model. An application of the method is independent on configuration of initial and boundary conditions.

The weak point of the method is the comparatively low accuracy of the measurement made by the IR camera.

The representative example and the IR camera image processing procedures are briefly described in the paper.

Acknowledgement:

The work was supported by the grant "Simulation of Modern Sensors' Electronic Thermal Load" No.102/06/0498, of the Czech Science Foundation.

References:

[1] Canny J.: *A Computational Approach to Edge Detection*. IEEE Transactions on Pattern Analysis and Machine Intelligence, Vol. 8, No. 6, November 1986. ISSN 0162-8828.

[2] Gonzalez R., Woods R., Eddins R.: *Digital Image Processing Using Matlab*. Prentice Hall. 2004. ISBN 0-13-008519-7.

[3] Haberman R.: Applied partial Differential Equations with Fourier Series and Boundary Value Problems. Fourth Edition. Pearson Prentice Hall. New Jersey 2004. ISBN 0-13-065243-1.

[4] Jain A. K.: *Fundamentals of Digital Image Processing*. Prentice Hall, New York 1989, ISBN 0-13-336165-9.

[5] Jaluria Y., Torreance K.E.: *Computational Heat Transfer*. Taylor and Francis, New York, 2003 ISBN 1-56932-477-5.

[6] Kazakov V. A., Rodriguez D.S.: *Reconstruction of Gaussian Regular Sampled Fields with Jitter*. WSEAS Transactions on Systems, Issue 8, Vol.5, August 2006. ISSN 1109-2777.

[7] Madeci E., Guven I.: *The Finite Element Method and Applications in Engineering Using ANSYS.* Springer, New York 2006, ISBN 0-387-28289-0.

[8] Nevriva P., Plesivcak P.: *Intelligent Simulation of Thermal Load of Sensors.* Proceedings of the 7th International Conference on Intelligent Systems Design and Applications ISDA 2007, Rio de Janeiro, Brazil, October 2007, ISBN 0-7695-2976-3 ISBN 978-0-7695-2976-9.

[9] Nevriva P., Plesivcak P., Grobelny D.: *Experimental Validation of Mathematical Models of Heat Transfer Dynamics of Sensors.* WSEAS Transactions on Systems, Issue 8, Vol.5, August 2006. ISSN 1109-2777.

[10] Nevriva P., Plesivcak P., Grobelny D.: *Simulation and experimental verification of heat transfer dynamics of sensors*. 10th WSEAS Int. Conf. on SYSTEMS 2006, Athens , Greece, 2006, ISBN 960-8457-47-5

[11] Saeed V. Vaseghi: *Advanced Digital Signal Processing and Noise Reduction.* Third Edition. John Wiley & Sons, Ltd. New York, 2006, ISBN 13978-0-470-09494-5.

[12] Saleh M. M., El-Kalla I. L., Ehab M. M. *Stochastic Finite Element for Stochastic Linear and Nonlinear Heat Equation with Random Coefficients.* WSEAS Transactions on Mathematics, Issue 12, Vol.5, December 2006, ISSN 1109-2769.

[13] Dmytruk I: *Integrating Nonlinear Heat Conduction Equation with Source Term.* WSEAS Transactions on Mathematics, Issue 1, Vol.3, January 2004, ISSN 1109-2769.